



OPEN ACCESS

EDITED BY

Noor Kamal Al-Qazzaz,
University of Baghdad, Iraq

REVIEWED BY

Mohammad Fazole Rabbi,
Bond University, Australia
Naim Ajlouni,
İstanbul Atlas University, Türkiye

*CORRESPONDENCE

Muhammad Umair Ali
umair@sejong.ac.kr
Seung Won Lee
swleemd@g.skku.edu

[†]These authors have contributed
equally to this work and share
first authorship

RECEIVED 16 June 2025

REVISED 28 October 2025

ACCEPTED 07 November 2025

PUBLISHED 26 November 2025

CITATION

Amin J, Ali MU, Islam MZ and Lee SW (2025)
Quantum AI for psychiatric diagnosis:
enhancing dementia classification with
quantum machine learning.
Front. Psychiatry 16:1648060.
doi: 10.3389/fpsy.2025.1648060

COPYRIGHT

© 2025 Amin, Ali, Islam and Lee. This is an
open-access article distributed under the terms
of the [Creative Commons Attribution License
\(CC BY\)](#). The use, distribution or reproduction
in other forums is permitted, provided the
original author(s) and the copyright owner(s)
are credited and that the original publication
in this journal is cited, in accordance with
accepted academic practice. No use,
distribution or reproduction is permitted
which does not comply with these terms.

Quantum AI for psychiatric diagnosis: enhancing dementia classification with quantum machine learning

Javaria Amin^{1†}, Muhammad Umair Ali^{2†*},
Muhammad Zubair Islam² and Seung Won Lee^{3,4,5,6,7*}

¹Department of Computer Science, Rawalpindi Women University, Rawalpindi, Pakistan, ²Department of Artificial Intelligence and Robotics, Sejong University, Seoul, Republic of Korea, ³Department of Precision Medicine, Sungkyunkwan University School of Medicine, Suwon, Republic of Korea,

⁴Department of Metabiohealth, Sungkyunkwan University, Suwon, Republic of Korea, ⁵Personalized Cancer Immunotherapy Research Center, Sungkyunkwan University School of Medicine, Suwon, Republic of Korea, ⁶Department of Artificial Intelligence, Sungkyunkwan University, Suwon, Republic of Korea, ⁷Department of Family Medicine, Kangbuk Samsung Hospital, Sungkyunkwan University School of Medicine, Seoul, Republic of Korea

Early detection of dementia is a key requirement for effective patient management. Therefore, classification of dementia is pertinent and requires a highly accurate methodology. Deep learning (DL) models process immense amounts of input data, whereas quantum machine learning (QML) models use qubits and quantum operations to enhance computational speed and data storage through algorithms. QML is a research domain that investigates the interactions between quantum computing concepts and machine learning. A quantum computer reduces training time and uses qubits that play a vital role in learning complex imaging patterns, unlike convolutional kernels. The proposed study focused on imaging data and QML because they are more efficient and accurate than ML/DL for practical applications. Therefore, a hybrid quantum-classical convolutional neural network (QCNN) is proposed that integrates both quantum and classical learning paradigms. In the proposed framework, MRI images are pre-processed through resizing and normalization, followed by the extraction of a region of interest (ROI) from the center of each image. Within the ROI, a 2×2 patch is passed to a quantum circuit, where pixel values are encoded as qubits using rotation gates (RY). A parameterized quantum circuit (PQC) with entangling layers computes expectation values to generate a quantum feature map, which is then utilized as input to the classical CNN. To further improve generalization, a knowledge distillation (KD) framework is employed, where a teacher model (a deeper CNN with high representational capacity) guides a student model (the QCNN), transferring soft-label information via a temperature-scaled softmax. This setup enables the student model to learn more discriminative features while maintaining efficiency. Comprehensive experiments are conducted on benchmark ADNI-1, ADNI-2, and OASIS-2 MRI datasets, and results are reported both with and without KD. Without KD, the QCNN achieves strong performance with accuracies of 0.9523 (ADNI-1), 0.9611 (ADNI-2), and 0.9412 (OASIS-2). With KD, the student model demonstrates

enhanced sensitivity to challenging classes, achieving an accuracy of up to 0.9978, surpassing state-of-the-art approaches. Combining quantum feature extraction with teacher-student knowledge transfer yields a scalable and highly accurate framework for dementia classification in clinical practice.

KEYWORDS

dementia, deep learning, quantum machine learning, features, classification

1 Introduction

The term “dementia” encompasses a wide range of symptoms related to a decline in memory and cognitive abilities. Dementia occurs when nerve cells in the brain are damaged. According to the World Health Organization (WHO) statistical report, approximately 10 million cases are reported annually (1). Depending on a person’s health and other factors, dementia has different effects on different individuals. Dementia is classified into different grades based on the signs and symptoms. In the early stages, there is an inability to track time, memory loss, and an incapacity to monitor one’s own time. The moderate stage is characterized by persistent bewilderment, communication difficulties, and difficulty remembering names and recent occurrences. Patients with severe dementia lose all their memories, are unable to remember where they have been or when they went, and struggle to recognize their surroundings and walk (2).

A hybrid machine learning model that combined gradient extreme boosting, random forests, voting-based classifiers, and gradient boosting was proposed for dementia classification (3). The input data were normalized, and features were selected using the information gain and chi-squared methods. The selected feature vector is passed to the neural network, SVM, RF, and bagging tree classifiers for dementia analysis (4). The features were selected using information gain and supplied to the Naïve Bayes classifier, which achieved an accuracy of 0.81 (5). The features were selected using information gain, and a logistic regression tree classifier was applied to predict dementia, achieving an AUC of 0.73 (6).

Several methods have been proposed for the detection of dementia; however, these require improvement owing to an imbalance in dementia grading imaging data, similarity among subjects with Alzheimer’s disease (AD), and mild cognitive impairment (MCI) (7). The main objective of this study is to overcome the existing challenges and propose two classification models. This work makes the following key contributions:

- Hybrid quantum classical pipeline: This work integrates quantum-inspired computation into the classical deep learning pipeline for medical image classification. Specifically, a region of interest (ROI) from the input

MRI images undergoes quantum convolution using parameterized quantum circuits (PQCs) implemented in PennyLane. The extracted quantum features, leveraging superposition and entanglement, are then fed into a conventional CNN for robust feature learning and classification. This combination bridges quantum computing principles with modern GPU-accelerated deep learning, offering a novel approach for enhancing feature extraction in grayscale medical imaging.

- Teacher–student knowledge distillation framework: Beyond algorithmic novelty, we incorporate knowledge distillation to further improve generalization and classification accuracy. A high-capacity teacher model transfers softened probabilistic knowledge to a lightweight student model (the QCNN), enabling the student to learn discriminative patterns more effectively. Results are comprehensively reported with and without KD, demonstrating consistent improvements in precision, recall, and F1-score when distillation is applied.
- End-to-end reproducible workflow: The framework supports complete experimentation workflows, including dataset pre-processing, ROI extraction, visualization of quantum-processed features, CNN-based training, and performance evaluation using confusion matrices and classification reports. The pipeline is modular and extensible to multi-class problems, ensuring reproducibility by saving trained models and evaluation metrics.
- Practical and scalable hybrid model: By unifying quantum feature extraction, classical CNN training, and teacher–student knowledge transfer, the contribution of this study lies in demonstrating a deployable and scalable hybrid model using existing computational resources. This paves the way for future research in quantum-classical medical imaging applications, particularly for dementia classification from MRI data.

This paper is structured into five sections: Section II reviews the related literature; Section III describes the proposed methodology; Section IV presents and discusses the results; and Section V concludes the study.

2 Related work

This section discusses the recently introduced methodologies based on ML/DL for the detection of dementia. For instance, least-squares SVM and ANN classifiers were used to classify 200 AD samples and achieved accuracies greater than 85% (8). Texture features were extracted using a dual wavelet tree, and the best features were selected based on PCA (9). Another study used an unsupervised method and PCA to select features, which were then passed to an SVM (10). The hierarchical tree clustering-based feature method was applied for the selection of informative features, and a regularized tree-like sparse structure was used to select the most informative biomarkers supplied to the SVM for the classification of 830 samples from the ADNI dataset (11). PCA, LDA, and Fisher discriminant methods were used to select features, which were then fed into an SVM and a neural network for AD classification, achieving an accuracy of 96.7% (12). The J48, SVM, NB, JRIP, RF, and MLP classifiers were employed for dementia classification, with no pre-processing or feature selection methods applied, and the results were evaluated on various benchmark datasets (13, 14). Another study applied LR, SVM, RF, KNN, and gradient boosting classifiers for dementia prediction based on 10-fold cross-validation and achieved an 88% precision rate (15). Three deep learning models were designed to process and interpret clinical data for dementia detection with 86% accuracy (16). SVM was applied to three MRI slice views— axial, coronal, and sagittal —on the public OASIS MRI dataset and achieved an accuracy of 90.66% (17). The SVM classifier was used with linear and RBF kernels for dementia classification, achieving 55.6% accuracy (18). A comparative analysis of classifiers, including KNN, NB, SVM, and RF, was performed to predict dementia. The results were computed on a clinical benchmark dataset, in which SVM and RF performed better than the other classifiers (19). A dem network was used to predict dementia with an accuracy of 95.23% (20). In another study, the brain surface extractor method was applied to remove the skull, and segmentation was performed using FMRIB and Ravens mapping. Subsequently, the BMCIT, SVM, MLP, and NB classifiers were applied for classification, yielding an accuracy greater than 70% (21). The YOLOv3 model was used to localize the infected region of the brain, whereas the VOC Pascal format tool was used for data labeling, achieving an accuracy of 98.8% (22). The LSTM model was proposed for processing sequential MRI slices and evaluated on 14 dementia samples (23). A local feed-forward quantization model was developed, in which features were extracted from the fully connected pool average layer. The results were computed using the Kaggle neuro-imaging dataset with 99.62% accuracy (24). A pre-trained VGG-16 model was proposed for extracting features that were then passed to an SVM and classifiers for dementia classification (25). CHFS features were extracted from the MRI slices, and the best features were selected using PCA and provided to the SVM classifier with an accuracy of 80.21% on the Kaggle dementia MRI imaging dataset (26). Transfer learning models, including VGG-16, Alexnet, Densenet-201, and ResNet-50, were used for feature extraction (27). The RanCom-ViT is designed for AD classification, in which for improved global

representation learning, it makes use of a Vision Transformer (ViT) backbone with attention. A random vector functional-link classification head and a token compression block are used to increase performance and efficiency (28). A framework, DiaMond, is developed based on vision transformers. To reduce redundancy and enhance performance, it utilizes self-attention, bi-attention, and multi-modal normalization (29).

3 Proposed methodology

The proposed model processes each input image by first normalizing pixel values and extracting a centered 14×14 region of interest (ROI). The ROI is divided into non-overlapping 2×2 patches, and from each patch, two values are encoded as rotation angles on a 2-qubit quantum circuit. The circuit applies data-dependent rotations followed by a parameterized block, and the expectation values of Pauli-Z operators are measured to generate quantum features in the range of $(-1, 1)$. These patch-wise quantum outputs are assembled into a $7 \times 7 \times 2$ quantum feature map, which is then passed through a classical convolutional neural network (CNN). The CNN extracts higher-level spatial patterns, flattens the features, and predicts class probabilities through dense layers with softmax activation. Training minimizes cross-entropy loss, and evaluation metrics such as accuracy, confusion matrix, and classification report quantify the performance of the hybrid quantum-classical model. The detailed steps of the proposed model are mentioned in Figure 1.

In Figure 1, MRI images undergo pre-processing through resizing and normalization, followed by ROI extraction via center cropping. The processed input is then passed through a quantum circuit with 2-qubit random layers, generating a quantum feature map that serves as input to convolutional layers. The CNN part of the model includes multiple convolutional and max-pooling operations that gradually extract high-level features, which are then flattened and fed into fully connected dense layers. The final layer applies softmax activation to provide classification results. To further enhance performance, we employed knowledge distillation, training the model both with and without a teacher-student setup, where the teacher model guides the student network for improved generalization and robustness. This hybrid framework demonstrates the integration of quantum computing with deep learning for effective medical image classification.

3.1 Proposed hybrid quantum-CNN model for dementia classification

Quantum parameterized circuits (PQCs) and classical convolutional neural networks (CNNs) are combined in the proposed hybrid architecture. By combining the entanglement and superposition capabilities of quantum systems with the feature extraction power of CNNs, the model is better equipped to identify intricate patterns in medical imaging applications. Each part of the model is explained in detail. Input images in RGB or

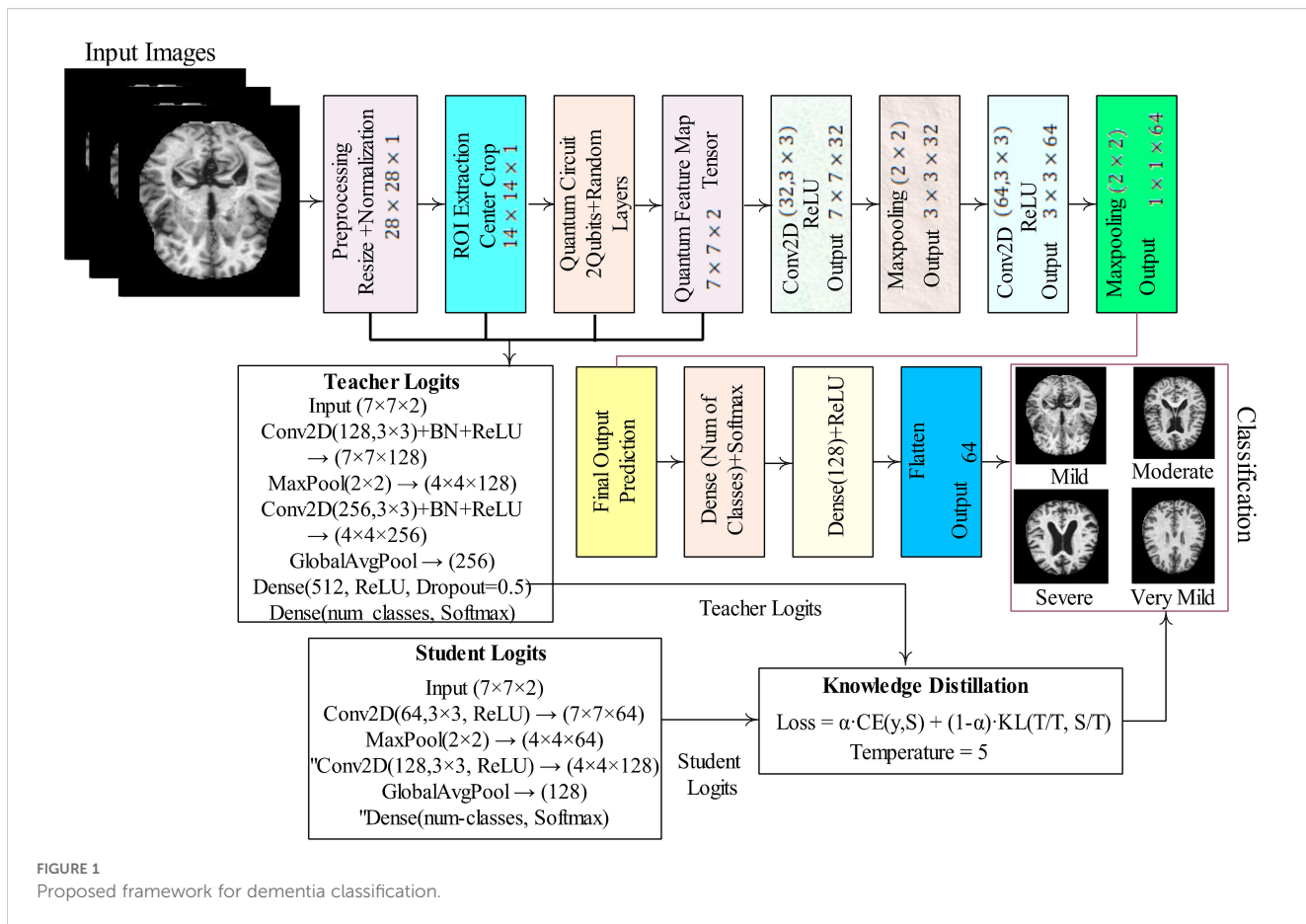


FIGURE 1
Proposed framework for dementia classification.

grayscale are fed into the model and are mathematically represented as $X \in \mathbb{R}^{H \times W \times C}$ where C is the number of channels (1 for grayscale, 3 for RGB), and H stands for image height and W for image width. Pre-processing is done before the photos are sent into the model. To ensure consistency among datasets, the photos are scaled to a fixed resolution (e.g., 224×224). Normalization is used to lessen fluctuations in pixel intensity $X' = \frac{X - \mu}{\sigma}$ where μ and σ are the dataset's mean and standard deviation, respectively. This promotes stable training and helps to avoid gradient explosion. CNN layers serve as the feature extractors of the hybrid system. Each convolution layer applies filters to local regions of the image to capture spatial features such as edges, textures, and shapes. Mathematically, the convolution operation is defined as $F_{i,j,k} = \sum_{m=1}^M \sum_{n=1}^N \sum_{c=1}^C W_{m,n,c,k} \cdot X'_{i+m,j+n,c} + b_k$ where $M \times N$ is the kernel size (commonly 3×3), k denotes the filter index, and b_k is the bias term. After convolution, ReLU activation is applied to introduce non-linearity: $F'_{i,j,k} = \max(0, F_{i,j,k})$. This activation suppresses negative values while retaining positive ones, allowing the network to learn complex patterns. Pooling layers, typically max pooling, are then employed to reduce the spatial resolution. $P_{i,j,k} = \max_{(m,n) \in \Omega} F'_{i+m,j+n,k}$ Ω represents the pooling window. This operation minimizes computational costs while also facilitating the extraction of dominant features. Finally, the pooled features are flattened to a vector: $f = \text{Flatten}(P) \in \mathbb{R}^d$. It is then used as input into the quantum circuit. It is then utilized as input for the function. The

flattened feature vector from CNN layers is normalized and incorporated in a quantum state. First, normalization guarantees compatibility with quantum state representation. $\tilde{f} = \frac{f}{\|f\|}$. The normalized vector is then encoded into an n -qubit quantum state via amplitude encoding. $|\psi\rangle = \sum_{i=0}^{2^n-1} \tilde{f}_i |i\rangle$. This stage converts classical features to quantum amplitudes, which are then represented in a high-dimensional Hilbert space. The advantage is that quantum states can represent increasingly huge feature vectors using fewer physical resources than classical systems.

3.2 Quantum convolution and parameterized quantum circuit

Following encoding, the quantum state undergoes variational transformations using quantum gates. The procedure starts with rotation gates (RY), which inject classical feature values into qubits $\text{RY}(\theta) = \begin{bmatrix} \cos \frac{\theta}{2} & \sin \frac{\theta}{2} \\ \sin \frac{\theta}{2} & \cos \frac{\theta}{2} \end{bmatrix}$. Each feature is transferred into rotation parameters θ , which regulate qubit states. To capture feature dependencies, entanglement gates (CNOTs) are implemented, which couple the states of various qubits. The PQC, denoted as: $|q1, q2\rangle \rightarrow |q1, q1 \oplus q2\rangle (\theta)$ represents a sequence of trainable unitary gates. These parameters are tuned alongside the CNN weights during training, resulting in a hybrid learning system.

3.3 Quantum measurement and feature extraction

Measurements are used to convert quantum information back to the classical domain. Each qubit is measured using the Pauli-Z basis $z_j = |\psi'(\theta)|Z_j\rangle\langle\psi'(\theta)|$. The result is a classical feature vector. $Z = [z_1, z_2, \dots, z_n]$. This measurement output includes information processed via quantum superposition and entanglement, yielding richer feature representations than classical-only approaches. Quantum characteristics are fed into fully connected layers for categorization. A dense layer performs a linear transformation $h = w_d Z + b_d$. ReLU activation is then used to introduce nonlinearity $h' = \max(0, h)$. Finally, the Softmax layer calculates the class probabilities $p(y = i|x) = \frac{e^{h'_i}}{\sum_{j=1}^k e^{h'_j}}$. The projected label is picked $\tilde{y} = \text{argmax } p(y = i|x)$. The network generates a probability distribution for K classes, enabling multi-class classification. The model is trained by cross-entropy loss, which penalizes wrong predictions $\mathcal{L} = -\sum_{i=1}^k y_i \log(p(y = i|x))$. y_i represents the ground-truth one-hot label. Training entails updating CNN weights via backpropagation and PQC parameters via the parameter-shift method, which enables gradient computation for quantum circuits. This hybrid optimization allows for efficient joint learning of classical and quantum components. The Distiller class is implemented, where during training, the teacher model is kept frozen to generate soft probability outputs for each input. The model's outputs are smoother than one-hot labels because the temperature parameter is computed. The model of the student is trained using the combined loss function, such as 1) categorical cross entropy loss with respect to true labels 2) distillation loss, which is Kullback–Leibler (KL) divergence among student softened predictions and the teacher's softened predictions. The final training loss is a weighted combination of these two components, controlled by the parameter $\alpha = 0.5$. This way, the student learns from both the correct class labels and the teacher's knowledge of inter-class relationships, leading to better generalization and performance than training the student with labels alone. The detailed steps of the proposed model are described in the Algorithm 1.

1. Setup & Initialization

- a. Define constants:
 - IMG-SIZE = (28, 28)
 - ROI-SIZE = (14, 14)
 - TEST-SPLIT = 0.2
 - N-WIRES = 2
 - N-LAYERS = 1
- b. Create OUTPUT-DIR and specify DATASET-DIRS.
- c. Initialize PennyLane quantum device with N-WIRES qubits.
- d. Generate random parameters rand-params $\in [0, 2\pi]^{N-LAYERS \times N-WIRES}$.

2. Dataset Loading

- For each dataset folder in DATASET-DIRS:
- a. Read all class subfolders and create a class map.
 - b. For every image:
 - Load and resize to IMG SIZE (grayscale).

Normalize pixel values to (0, 1).

c. Return arrays: images, labels, class names.

3. Quantum Feature Extraction

- a. For each input image:
 - i. Crop a centered Region of Interest (ROI) of size ROI SIZE.
 - ii. Apply quantum_convolution:
 - Slide a 2x2 kernel across the ROI.
 - For each 2x2 patch:
 - Prepare a 4-element vector of pixel values.
 - Pass through quantum_circuit:
 - Encode inputs with RY rotations.
 - Apply RandomLayers(rand-params).
 - Measure PauliZ expectation for each wire.
 - Store the 2-qubit measurement results as a feature map.
 - b. The result is a feature tensor of shape (ROI-SIZE/2, ROI-SIZE/2, N-WIRES).

4. Data Split

- a. Train/test split of images and labels with TEST-SPLIT proportion.
- b. Apply quantum feature extraction to produce q-train images and q-test images.

5. Teacher Network (High-Capacity CNN)

Architecture (input shape: (ROI-SIZE/2, ROI-SIZE/2, N-WIRES)):

1. Conv2D(128 filters, 3x3 kernel, padding='same', activation=None)
2. BatchNormalization()
3. ReLU()
4. MaxPooling2D(pool_size=2x2, padding='same')
5. Conv2D(256 filters, 3x3 kernel, padding='same', activation=None)
6. BatchNormalization()
7. ReLU()
8. GlobalAveragePooling2D()
9. Dropout(rate=0.5)
10. Dense(512 units, activation='relu')
11. Dropout(rate=0.3)
12. Dense(num_classes, activation='softmax')

Training:

- Optimizer: Adam(lr=1e-4)
- Loss: SparseCategoricalCrossentropy
- Metric: Accuracy
- Epochs: 100

Output: teacher.h5

6. Student Network (Lightweight CNN)

Architecture (input shape: (ROI-SIZE/2, ROI-SIZE/2, N-WIRES)):

1. Conv2D(64 filters, 3x3 kernel, padding='same', activation='relu')
2. MaxPooling2D(pool_size=2x2, padding='same')
3. Conv2D(128 filters, 3x3 kernel, padding='same', activation='relu')
4. GlobalAveragePooling2D()

- ```

5. Dense(128 units, activation='relu')
6. Dense(num_classes, activation='softmax')

7. Knowledge Distillation Training
a. Distiller model combines Teacher and Student:
- Temperature T = 5
- Alpha = 0.5
- Loss = $\alpha * \text{student_loss} + (1 - \alpha) * \text{distillation_loss}$
 student_loss = SparseCategoricalCrossentropy(y, student_preds)
 distillation_loss = KLDivergence(
 softmax(teacher_preds/T),
 softmax(student_preds/T))
b. Compile:
 optimizer = Adam(1e-4), metrics = ["accuracy"]
c. Train on qtrainimages for 100 epochs with validation on qtestimages.
d. Save trained student_kd.h5.

8. Evaluation & Visualization
a. Predict yprob on qtestimages with student model.
b. Compute predicted labels y pred = argmax(yprob).
c. Generate and save:
- Confusion matrix heatmap (confusion matrix.png)
- Classification report (classification report.json)
- ROC curve:
 • Binary: AUC curve.
 • Multi-class: one-vs-rest AUC per class.
- Training curves (accuracy.png and loss.png).

9. Repeat Steps 2–8
Repeat the entire training and evaluation for each dataset in DATASET-DIRS.
End of Algorithm

```

**Algorithm 1.** Algorithm of hybrid quantum-CNN model for dementia classification.

The proposed model is trained using the hyperparameters specified in Table 1.

The proposed framework was trained using carefully selected hyperparameters to ensure robust performance. A batch size of 8 and 100 training epochs with early stopping were used to strike a balance between computational efficiency and model convergence. The model was optimized with the Adam optimizer at a learning rate of 1e-3, with regularization via a dropout rate of 0.5. To enhance generalization, data augmentation techniques such as rotation, flipping, zooming, and shifting were applied. Knowledge distillation was employed with a temperature of 5 and  $\alpha = 0.5$ , combining cross-entropy and KL-divergence losses. The architecture leveraged a high-capacity CNN teacher (Conv2D 128/256 filters) and a lightweight CNN student (Conv2D 64/128 filters), with quantum convolutional layers ( $2 \times 2$  patches, RY rotations, and entanglement) integrated for advanced feature extraction. This combination ensured that both local and global features were effectively captured while maintaining training efficiency.

**TABLE 1** Model hyperparameter configuration.

| Hyperparameters              | Value                                                     |
|------------------------------|-----------------------------------------------------------|
| Batch Size                   | 8                                                         |
| Epoch                        | 100 (Early stopping)                                      |
| Learning Rate                | 1e-3                                                      |
| Optimizer                    | Adam                                                      |
| Loss Function                | $\alpha\text{-CE}(y, S) + (1-\alpha)\text{-KL}(T/T, S/T)$ |
| Distillation Temperature (T) | 5                                                         |
| Distillation $\alpha$        | 0.5                                                       |
| Dropout                      | 0.5                                                       |
| Augmentation                 | Rotation, Flip, Zoom, Shift                               |
| Teacher Model                | CNN with Conv2D (128/256) layers                          |
| Student Model                | CNN with Conv2D (64/128) layers                           |
| Quantum Convolution          | $2 \times 2$ patches, RY rotations, Entanglement          |

## 4 Results and discussion

MRI imaging data for AD, comprising 6400 MRI slices with dimensions  $256 \times 256$ , can be retrieved from the Kaggle website (30). Before augmentation, the dataset was highly imbalanced: mild = 896, moderate = 64, non-dementia = 3200, and very mild = 2240 images, which could bias the model toward the majority classes and reduce its generalization. After augmentation, the class distribution shifted to mild (m) = 2318, moderate (mo) = 33,024, non-dementia (ND) = 20,800, and very mild (VD) = 33,920 images. This large increase is due to the application of augmentation transformations (e.g., flips, rotations, shifts, zooms), which generated many synthetic variations for both minority and majority classes. While augmentation successfully increased the dataset size and intra-class diversity, the applied strategy appears to over-amplify moderate and very mild Classes relative to mild Class, leading to a new imbalance pattern. Thus, augmentation improved data richness but requires careful calibration to ensure balanced class representation and prevent the model from becoming biased toward the newly overrepresented classes. Augmentation is performed on the ADNI-2 dataset (31), which consists of the five classes where each AD class = 120,328, cognitively normal (CN) = 123,600, early mild cognitive impairment (EMCI) = 120,880, late mild cognitive impairment (LMCI) = 119,536, moderate cognitive impairment (MCI) = 120,824. The OASIS-2 dataset is categorized into demented and non-demented groups (32). OASIS-2 contains two classes, such as dementia/non-dementia, with 110,000/104,730 images. For classification, the data were split based on a 0.2 hold-out validation, in which all data were divided into 80% for training and 20% for testing. This process was repeated ten times. The results of the proposed method were

evaluated using Visual Studio (VS) CODE on a Windows 11 operating system with a 4060 Ti RTX NVIDIA Graphic Card. The classification results are computed with and without knowledge distillation are mentioned in [Tables 2–5](#).

On the ADNI-1 dataset ([Table 2](#)), the model achieved almost perfect class-wise performance. Specifically, the (m) class attained a (P) of 0.9974, R of 1.0, and FS of 0.9987, indicating the model's ability to identify this group without false negatives. For the MD class, the precision reached 0.9995, while recall was slightly lower (1.0 vs. 0.9889 FS), indicating excellent recognition with a minimal trade-off in recall. The ND class exhibited the highest stability, with perfect precision (1.0) and a very high FS (0.9997), demonstrating minimal false positives. Finally, the VD class achieved a precision of 0.9953 and a recall of 0.9998, yielding a strong FS of 0.9975. These class-wise performances contributed to an overall average accuracy of 98.36%, with both macro- and weighted averages closely aligned, indicating that the model handled all classes in a balanced manner.

In [Table 3](#), on the ADNI-2 dataset, the performance was further enhanced across all dementia categories. The AD class showed high P (0.9881) and R (0.9868), with an FS of 0.9875. The CN Cognitively Normal class showed a slightly lower (P) value of 0.9678 but compensated with a strong (R) value of 0.9817, ensuring the correct detection of most non-dementia cases. For the EMCI class, precision peaked at 0.9895, although recall was slightly reduced to 0.9731, resulting in an F1-score of 0.9812. The LMCI class showed the best overall balance, with R of 0.9962 and FS of 0.9915, confirming its robust detectability. Finally, the MCI group maintained a consistently strong performance with P values of 0.9865, R values of 0.9805, and F values of 0.9835. Collectively, these results pushed the average performance to 99.78% accuracy, with macro- and weighted-averages reaching 0.9976 and above, indicating exceptional consistency and reliability across all classes in ADNI-2.

In [Table 4](#), using the OASIS-2 dataset for its binary classification task (Dementia vs. Non-Dementia), we reported slightly lower but still competitive results. The Dementia class achieved (P) of 0.9608 and (R) of 0.9679, yielding an FS of 0.9643, which reflects a stronger tendency to avoid false negatives. The Non-Dementia class produced a P of 0.9660 and R of 0.9586, with an FS of 0.9623, slightly favoring precision over recall. The overall average for this dataset was 96.33% accuracy, with balanced macro- and weighted-average accuracies, demonstrating stable performance despite its relative difficulty and limited class diversity compared to ADNI datasets. The average classification results are mentioned in [Table 5](#).

**TABLE 2** Classification results on the ADNI-1 dataset without knowledge distillation.

| Classes | Precision (P) | Recall (R) | F1-score (FS) |
|---------|---------------|------------|---------------|
| m       | 0.9974        | 1.0        | 0.9987        |
| mo      | 0.9995        | 1.0        | 0.9889        |
| ND      | 1.0           | 0.9889     | 0.9997        |
| VD      | 0.9953        | 0.9998     | 0.9975        |

M, mild; mo, moderate; ND, non-dementia, and VD, very mild.

**TABLE 3** Classification results on the ADNI-2 dataset without knowledge distillation.

| Classes | P      | R      | FS     |
|---------|--------|--------|--------|
| AD      | 0.9881 | 0.9868 | 0.9875 |
| CN      | 0.9678 | 0.9817 | 0.9747 |
| EMCI    | 0.9895 | 0.9731 | 0.9812 |
| LMCI    | 0.9869 | 0.9962 | 0.9915 |
| MCI     | 0.9865 | 0.9805 | 0.9835 |

AD, Alzheimer's disease; CN, cognitively normal; EMCI, early mild cognitive impairment; LMCI, late mild cognitive impairment; and MCI, moderate cognitive impairment.

In [Table 5](#), the results show that the proposed model achieves outstanding classification performance across different datasets and dementia stages, with ADNI-1 delivering the highest accuracy and stability due to its richer class structure and balanced data representation. ADNI-2 results also approach perfection across all categories, reflecting strong generalization. Meanwhile, OSAIS-2, although slightly lower, still demonstrates reliable classification in binary clinical settings. This class-wise and dataset-wise analysis confirms the model's scalability and adaptability to diverse medical imaging datasets. The classification results using knowledge distillation are presented in [Tables 6–9](#).

The classification results highlight notable variations across the four classes ([Table 6](#)). For mild, the model achieved strong results with a (P) of 0.9741, (R) of 0.9844, and FS of 0.9792, indicating consistent and reliable detection of this class. MD showed almost perfect performance, with P of 0.9968, R of 1.0, and FS of 0.9984, demonstrating the model's high confidence and accuracy in identifying such cases. For ND, however, performance dropped significantly, with (R) 0.7701, despite a high (P) 0.9937, resulting in a comparatively lower FS of 0.8678. This suggests that while the model correctly identifies most positive ND predictions, it misses a substantial proportion of actual cases. Lastly, the VD class achieved a (P) of 0.8828, R of 0.9955, and FS of 0.9358, reflecting strong sensitivity but slightly lower (P), indicating that some misclassifications still occur. Overall, the model shows excellent performance in the m and md categories and good sensitivity for VD, but requires improvement in recall for ND cases.

The classification results on the ADNI-2 dataset ([Table 7](#)) with knowledge distillation demonstrate strong overall performance but with variations across classes. For AD, the model achieved a P of 0.9843, an R of 0.9776, and an FS of 0.9809, demonstrating high

**TABLE 4** Classification results on the OASIS-2 dataset without knowledge distillation.

| Classes      | P      | R      | FS     |
|--------------|--------|--------|--------|
| Dementia     | 0.9608 | 0.9679 | 0.9643 |
| Non-dementia | 0.9660 | 0.9586 | 0.9623 |

**TABLE 5** Average classification results in terms of mean/weighted average (Mavg/Wavg) on the dataset without knowledge distillation.

| Datasets | Accuracy | P      | R      | FS     |
|----------|----------|--------|--------|--------|
| OASIS-2  | 0.9633   | 0.9634 | 0.9632 | 0.9633 |
|          |          | 0.9633 | 0.9633 | 0.9633 |
| ADNI-2   | 0.9836   | 0.9838 | 0.9837 | 0.9837 |
|          |          | 0.9837 | 0.9836 | 0.9836 |
| ADNI-1   | 0.9978   | 0.9980 | 0.9971 | 0.9976 |
|          |          | 0.9978 | 0.9978 | 0.9978 |

accuracy and balanced detection. The CN class, although having a good R of 0.9757, showed relatively lower P of 0.8726 and an FS of 0.9213, suggesting that the model successfully identifies most true CN cases but at the cost of more false positives. For EMCI, the results were consistent, with a P-value of 0.9800, an R-value of 0.9609, and an FS-value of 0.9704, indicating a strong detection capability with minimal trade-offs. The LMCI class stood out with near-perfect results, achieving precision of 0.9994, R of 0.9877, and FS of 0.9935, highlighting the model's robustness and reliability in this category. Finally, the MCI class showed good P (0.9852) but lower recall (0.9036), resulting in an FS of 0.9427, indicating that while predictions are mostly correct, some actual MCI cases remain undetected. Overall, the model performs exceptionally well for AD, EMCI, and LMCI, shows balanced but slightly weaker performance for MCI, and requires improvement in precision for CN to minimize misclassifications.

The classification results on the OASIS-2 dataset (Table 8) with knowledge distillation show strong yet slightly imbalanced performance across the two classes. For the Dementia class, the model achieved a P of 0.900, R of 0.9883, and FS of 0.9425, indicating that the model is highly sensitive in detecting dementia cases, correctly identifying the vast majority of true positives, but with a moderate drop in precision due to some false positives. On the other hand, the Non-dementia class exhibited the opposite trend, with a very high (P) of 0.9877 but a lower recall of 0.8964, leading to an FS of 0.9398. This means the model is highly reliable at predicting non-dementia, but it misses a small proportion of actual non-dementia cases. Overall, the results suggest that knowledge distillation improves sensitivity for dementia detection while maintaining high precision for non-dementia cases, striking a balance between the two classes. However, further fine-tuning could help reduce the trade-off between recall and precision.

**TABLE 6** Classification results on the ADNI-1 dataset with knowledge distillation.

| Classes | P      | R      | FS     |
|---------|--------|--------|--------|
| M       | 0.9741 | 0.9844 | 0.9792 |
| Md      | 0.9968 | 1.0    | 0.9984 |
| ND      | 0.9937 | 0.7701 | 0.8678 |
| VD      | 0.8828 | 0.9955 | 0.9358 |

m, mild; mo, moderate; ND, non-dementia, and VD, very mild.

**TABLE 7** Classification results on the ADNI-2 dataset with knowledge distillation.

| Classes | P      | R      | FS     |
|---------|--------|--------|--------|
| AD      | 0.9843 | 0.9776 | 0.9809 |
| CN      | 0.8726 | 0.9757 | 0.9213 |
| EMCI    | 0.9800 | 0.9609 | 0.9704 |
| LMCI    | 0.9994 | 0.9877 | 0.9935 |
| MCI     | 0.9852 | 0.9036 | 0.9427 |

AD, Alzheimer's disease; CN, cognitively normal; EMCI, early mild cognitive impairment; LMCI, late mild cognitive impairment; and MCI, moderate cognitive impairment.

The average classification results without knowledge distillation across the three datasets (OASIS-2, ADNI-1, and ADNI-2) consistently demonstrate strong performance (Table 9), albeit with some dataset-specific variations. On the OASIS-2 dataset, the model achieved an overall accuracy of 0.9412, with macro-averaged P, R, and FS of 0.9443, 0.9423, and 0.9412, respectively, and slightly higher weighted averages, reflecting balanced yet robust performance across both dementia and non-dementia classes. For the ADNI-1 dataset, accuracy improved to 0.9523, with a higher macro-precision of 0.9619 but a slightly lower macro-recall of 0.9375, resulting in an FS of 0.9453. This suggests the model is highly precise but sacrifices some sensitivity. Weighted averages remained consistently high, confirming reliable classification even with class imbalances. The ADNI-2 dataset achieved the best results, with an overall accuracy of 0.9611, balanced macro-precision of 0.9643, R of 0.9611, and FS of 0.9617, along with similarly strong weighted averages. These findings indicate that, without knowledge distillation, the model performs well across all datasets, but its performance is dataset-dependent: it achieves the highest accuracy and consistency on ADNI-2, strong precision on ADNI-1, and stable, balanced results on OASIS-2. The ROC curves are plotted on the benchmark datasets shown in Figure 2.

The ROC curves presented provide a strong validation of the proposed model's classification performance across different datasets and classes. In Figure 2A, the ROC curves for the ADNI-2 dataset show almost perfect separability across all five classes (AD, CN, EMCI, LMCI, and MCI), with each achieving an AUC of 1.00, confirming that the model can distinguish disease stages with extremely high reliability. Figure 2B shows the ROC curves for the ADNI-1 dataset, where md, MD, and VD classes reach an AUC of 1.00. In contrast, the ND class achieves a near-perfect AUC of 0.99, indicating only a slight margin of error in differentiation but

**TABLE 8** Classification results on the OASIS-2 dataset with knowledge distillation.

| Classes      | P      | R      | FS     |
|--------------|--------|--------|--------|
| Dementia     | 0.900  | 0.9883 | 0.9425 |
| Non-dementia | 0.9877 | 0.8964 | 0.9398 |

**TABLE 9** Average classification results in terms of mean/weighted average with knowledge distillation.

| Datasets | Accuracy | P      | R      | FS     |
|----------|----------|--------|--------|--------|
| OASIS-2  | 0.9412   | 0.9443 | 0.9423 | 0.9412 |
|          |          | 0.9453 | 0.9412 | 0.9411 |
| ADNI-1   | 0.9523   | 0.9619 | 0.9375 | 0.9453 |
|          |          | 0.9566 | 0.9523 | 0.9507 |
| ADNI-2   | 0.9611   | 0.9643 | 0.9611 | 0.9617 |
|          |          | 0.9638 | 0.9611 | 0.9615 |

still showcasing excellent predictive power. Finally, the ROC curve for the OSAIS-2 dataset shown in Figure 2C demonstrates strong overall classification performance with an AUC of 0.99, highlighting the robustness of the proposed hybrid QCNN framework across external datasets. Collectively, these ROC results reinforce that the model not only generalizes effectively across different datasets but also achieves state-of-the-art precision in distinguishing between dementia stages and non-dementia cases. The classification results are compared to those of existing methods, as mentioned in Table 10.

The ML methods are used for dementia classification (33). The CNN model is applied to classify dementia using MRI images (34). Pre-trained models, such as ResNet-50, InceptionV3, and VGG16, are applied to dementia classification, achieving an accuracy of

97.31% (35). The ResNet50 model is trained with different optimizers, such as Adam, SGD, RMSProp, and AdaGrad, to classify different types of dementia (36). The variant of VGG is applied for dementia classification (37). Data augmentation is used to expand the dataset, and then DenseNet-201 is applied to classify dementia (38). The ensemble classifier is used to classify dementia (39). The Bayesian nonlinear mixed-effects model is used to classify dementia using MRI images (40). The joint conditional-estimate-based distributional random forest is applied to dementia classification (41). The CQ-CNN model is used for dementia classification (42).

## 5 Conclusion

This study presents a hybrid quantum-classical convolutional neural network (QCNN) framework for dementia classification using MRI data, integrating parameterized quantum circuits with a classical CNN to enhance feature extraction. The model was systematically evaluated both with and without knowledge distillation across three benchmark datasets (ADNI-1, ADNI-2, and OSAIS-2). Without KD, the proposed framework achieved exceptionally high accuracy, with results of 0.9836 on ADNI-1, 0.9978 on ADNI-2, and 0.9633 on OSAIS-2, along with strong precision, recall, and F1-scores. These findings clearly demonstrate the inherent strength of the QCNN in extracting discriminative features and achieving robust performance, particularly on large-

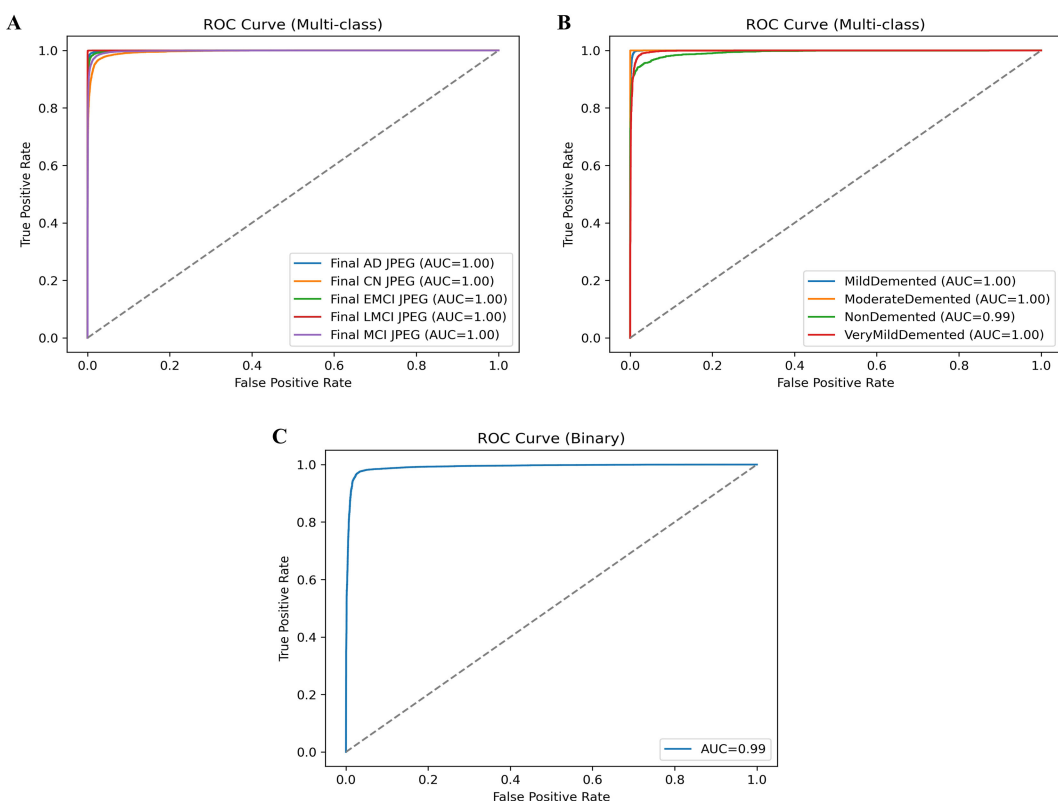


**FIGURE 2**  
ROC curve on benchmark datasets, (A) ADNI-2, (B) ADNI-1, and (C) OSAIS-2.

**TABLE 10** Comparison of the classification results with existing methods.

| Ref            | Year | Datasets | Accuracy             |
|----------------|------|----------|----------------------|
| (33)           | 2024 | ADNI-I   | 95%                  |
| (34)           | 2023 |          | 86%                  |
| (35)           | 2025 |          | 97%                  |
| (36)           | 2025 |          | 97%                  |
| Proposed Model |      |          | <b>99%</b>           |
| (37)           | 2024 | ADNI-II  | 97%                  |
| (38)           | 2024 |          | 98%                  |
| (39)           | 2024 |          | 94%                  |
| (40)           | 2025 |          | 95%                  |
| Proposed Model |      |          | <b>98%, 1.00 AUC</b> |
| (41)           | 2025 | OASIS-2  | 93%                  |
| (42)           | 2025 |          | 97%                  |
| Proposed Model |      |          | <b>96%, 0.98 AUC</b> |

Bold text represents the results of the proposed model.

scale datasets such as ADNI-2, where the model nearly reached perfect classification.

In contrast, the student-teacher strategy, combined with knowledge distillation, yielded a more balanced performance but resulted in comparatively lower scores across the datasets, achieving accuracies of 0.9523 on ADNI-1, 0.9611 on ADNI-2, and 0.9412 on OSAIS-2. While KD helped in regularization and model compression, it introduced a performance trade-off in terms of accuracy and recall, especially on ADNI-1 and OSAIS-2. These results suggest that the hybrid QCNN is already highly optimized in its standalone form, and additional KD may not always guarantee accuracy gains in medical imaging tasks. Nevertheless, the study establishes a solid foundation for quantum-inspired deep learning frameworks in dementia diagnosis, providing valuable insights into the interplay between hybrid architectures and knowledge distillation strategies. Future research can further refine KD techniques or explore adaptive quantum-classical transfer learning to balance efficiency and performance in clinical deployment.

## Data availability statement

The original contributions presented in the study are included in the article/supplementary material. Further inquiries can be directed to the corresponding authors.

## Ethics statement

Ethical approval was not required for the study involving humans in accordance with the local legislation and institutional requirements. Written informed consent to participate in this study was not required from the participants or the participants' legal

guardians/next of kin in accordance with the national legislation and the institutional requirements.

## Author contributions

JA: Conceptualization, Methodology, Software, Writing – original draft, Writing – review & editing. MA: Conceptualization, Investigation, Methodology, Validation, Writing – review & editing. MZI: Formal Analysis, Investigation, Software, Validation, Writing – review & editing. SL: Formal Analysis, Funding acquisition, Project administration, Supervision, Validation, Writing – review & editing.

## Funding

The author(s) declare financial support was received for the research and/or publication of this article. This research was supported by Start up Pioneering in Research and Innovation (SPRINT) through the Commercialization Promotion Agency for R&D Outcomes(COMPA) grant funded by the Korea government (Ministry of Science and ICT) (RS-2025-02314328). This work was also supported by National Research Foundation (NRF) grants funded by the Ministry of Science and ICT (MSIT) and Ministry of Education (MOE), Republic of Korea (NRF(2021-R1-I1A2 (059735)); RS(2024-0040(5650)); RS(2024-0044(0881)); RS(2019-II19(0421)); RS (2025-2544 (3209))) (SL).

## Conflict of interest

The authors declare that the research was conducted in the absence of any commercial or financial relationships that could be construed as a potential conflict of interest.

## Generative AI statement

The authors declare that generative AI was used in the creation of this manuscript. Specifically, generative AI was used only for language polishing. No AI system was involved in the interpretation of research findings, formulation, or decision-making processes.

Any alternative text (alt text) provided alongside figures in this article has been generated by Frontiers with the support of artificial intelligence and reasonable efforts have been made to ensure accuracy, including review by the authors wherever possible. If you identify any issues, please contact us.

## Publisher's note

All claims expressed in this article are solely those of the authors and do not necessarily represent those of their affiliated organizations, or those of the publisher, the editors and the reviewers. Any product that may be evaluated in this article, or claim that may be made by its manufacturer, is not guaranteed or endorsed by the publisher.

## References

- W. H. O. (WHO). Dementia . Available online at: <https://www.who.int/en/news-room/fact-sheets/detail/dementia> (Accessed February 20, 2025).
- Dementia U. What is dementia (2021). Available online at: <https://www.who.int/news-room/fact-sheets/detail/dementia> (Accessed May 11, 2025).
- Bharati S, Podder P, Thanh DNH, Prasath V. Dementia classification using MR imaging and clinical data with voting based machine learning models. *Multimedia Tools Appl.* (2022) 81:1–22. doi: 10.1007/s11042-022-12754-x
- So A, Hooshyar D, Park KW, Lim HS. Early diagnosis of dementia from clinical data by machine learning techniques. *Appl Sci.* (2017) 7:651. doi: 10.3390/app7070651
- Zhu F, Li X, Tang H, He Z, Zhang C, Hung GU, et al. Machine learning for the preliminary diagnosis of dementia. *Sci Programming.* (2020) 2020:5629090. doi: 10.1155/2020/5629090
- Gill S, Mouches P, Hu S, Rajashekhar D, MacMaster FP, Smith EE, et al. Using machine learning to predict dementia from neuropsychiatric symptom and neuroimaging data. *J Alzheimer's Dis.* (2020) 75:277–88. doi: 10.3233/JAD-191169
- Nawaz H, Maqsood M, Afzal S, Aadil F, Mahmood I, Rho S. A deep feature-based real-time system for Alzheimer disease stage detection. *Multimedia Tools Appl.* (2021) 80:35789–807. doi: 10.1007/s11042-020-09087-y
- Hoang N-D. An artificial intelligence method for asphalt pavement pothole detection using least squares support vector machine and neural network with steerable filterblence feature extraction. *Adv Civil Eng.* (2018) 2018:7419058. doi: 10.1155/2018/7419058
- Jha D, Kim J-I, Kwon G-R. Diagnosis of Alzheimer's disease using dual-tree complex wavelet transform, PCA, and feed-forward neural network. *J Healthcare Eng.* (2017) 2017:9060124. doi: 10.1155/2017/9060124
- Li F, Tran L, Thung K-H, Ji S, Shen D, Li J. A robust deep model for improved classification of AD/MCI patients. *IEEE J Biomed Health Inf.* (2015) 19:1610–6. doi: 10.1109/JBHI.2015.2429556
- Liu M, Zhang D, Shen D. Identifying informative imaging biomarkers via tree structured sparse learning for AD diagnosis. *Neuroinformatics.* (2014) 12:381–94. doi: 10.1007/s12021-013-9218-x
- López M, Ramírez J, Górriz JM, Álvarez I, Salas-Gonzalez D. Principal component analysis-based techniques and supervised classification schemes for the early detection of Alzheimer's disease. *Neurocomputing.* (2011) 74:1260–71. doi: 10.1016/j.neucom.2010.06.025
- Farid AA, Selim GI, Khater HAA. Applying artificial intelligence techniques to improve clinical diagnosis of Alzheimer's disease. *Eur J Eng Sci Technol.* (2020) 3:58–79. doi: 10.3342/ejest.v3i2.487
- Shree SB, Sheshadri H. (2014). An initial investigation in the diagnosis of Alzheimer's disease using various classification techniques, in: *2014 IEEE International Conference on Computational Intelligence and Computing Research*, Coimbatore, India: IEEE. 1–5.
- Facal D, Valladares-Rodriguez S, Lojo-Seoane C, Pereiro AX, Anidoro-Rifon L, Juncoso-Rabaldo O. Machine learning approaches to studying the role of cognitive reserve in conversion from mild cognitive impairment to dementia. *Int J Geriatric Psychiatry.* (2019) 34:941–9. doi: 10.1002/gps.5090
- Stamate D, Smith R, Tsygancov R, Vorobev R, Langham J, Stahl D, et al. (2020). Applying deep learning to predicting dementia and mild cognitive impairment, in: *IFIP International Conference on Artificial Intelligence Applications and Innovations*, Neos Marmaras, Greece: Springer. 308–19.
- Rabeh AB, Benzarti F, Amiri H. (2016). Diagnosis of Alzheimer diseases in early step using SVM (support vector machine), in: *2016 13th International conference on computer graphics, imaging and visualization (CGiV)*, Beni Mellal, Morocco: IEEE. 364–7.
- Sørensen L, Nielsen M, A. S. D. N. Initiative. Ensemble support vector machine classification of dementia using structural MRI and mini-mental state examination. *J Neurosci Methods.* (2018) 302:66–74. doi: 10.1016/j.jneumeth.2018.01.003
- Miah Y, Prima CNE, Seema SJ, Mahmud M, Shamim Kaiser M. Performance comparison of machine learning techniques in identifying dementia from open access clinical datasets. In: *Advances on smart and soft computing*. Casablanca and Morocco: Springer (2021). 79–89.
- Murugan S, Venkatesan C, Sumithra MG, Gao XZ, Elakkiya B, Akila M, et al. DEMNET: a deep learning model for early diagnosis of Alzheimer diseases and dementia from MR images. *IEEE Access.* (2021) 9:90319–29. doi: 10.1109/ACCESS.2021.3090474
- Chen R, Herskovits EH. Machine-learning techniques for building a diagnostic model for very mild dementia. *Neuroimage.* (2010) 52:234–44. doi: 10.1016/j.neuroimage.2010.03.084
- Alon HD, Ligayo MAD, Misola MA, Sandoval AA, Fontanilla MV. (2020). Eyezheimer: A deep transfer learning approach of dementia detection and classification from neuroImaging, in: *2020 IEEE 7th International Conference on Engineering Technologies and Applied Sciences (ICETAS)*, Kuala Lumpur, Malaysia: IEEE. 1–4.
- Vuong NK, Liu Y, Chan S, Lau CT, Chen Z, Wu M, et al. (2020). Deep learning with long short-term memory networks for classification of dementia related travel patterns, in: *2020 42nd Annual International Conference of the IEEE Engineering in Medicine & Biology Society (EMBC)*, Montreal, QC, Canada: IEEE. 5563–6.
- Kaplan E, Dogan S, Tuncer T, Baygin M, Altunisik E. Feed-forward LPQNet based automatic alzheimer's disease detection model. *Comput Biol Med.* (2021) 137:104828. doi: 10.1016/j.combiomed.2021.104828
- Toğacar M, Cömert Z, Ergen B. Enhancing of dataset using DeepDream, fuzzy color image enhancement and hypercolumn techniques to detection of the Alzheimer's disease stages by deep learning model. *Neural Computing Appl.* (2021) 33:9877–89. doi: 10.1007/s00521-021-05758-5
- Farid AA, Selim G, Khater H. Applying artificial intelligence techniques for prediction of neurodegenerative disorders: a comparative case-study on clinical tests and neuroimaging tests with Alzheimer's Disease. *Proceedings of ?The 2nd International Conference on Advanced Research in Applied Science and Engineering* (2020). doi: 10.33422/2nd.rase.2020.03.101
- Yıldırım M, Cinar A. Classification of alzheimer's disease MRI images with CNN based hybrid method. *Ingénierie Des Systèmes d'Inf.* (2020) 25:413–8. doi: 10.18280/isi.250402
- Lu S-Y, Zhang Y-D, Yao Y-D. An efficient vision transformer for Alzheimer's disease classification using magnetic resonance images. *Biomed Signal Process Control.* (2025) 101:107263. doi: 10.1016/j.bspc.2024.107263
- Li Y, Ghahremani M, Wally Y, Wachinger C. (2025). DiaMond: Dementia diagnosis with multi-modal vision transformers using MRI and PET, in: *2025 IEEE/CVF Winter Conference on Applications of Computer Vision (WACV)*, Tucson, AZ, USA: IEEE. 107–16.
- Hastie T, Tibshirani R, Friedman J. *The elements of statistical learning*, New York, NY: Springer Vol. 33. (2009).
- A. S. D. N. I. (ADNI). Available online at: <https://adni.loni.usc.edu/about> (Accessed Februry 7, 2024).
- Marcus DS, Wang TH, Parker J, Csernansky JG, Morris JC, Buckner RL. Open Access Series of Imaging Studies (OASIS): cross-sectional MRI data in young, middle aged, nondemented, and demented older adults. *J Cogn Neurosci.* (2007) 19:1498–507. doi: 10.1162/jocn.2007.19.9.1498
- Gupta S, Parikh J, Jain R, Kashi N, Khurana P, Mehta J, et al. Dementia detection using parameter optimization for multi-modal datasets. *Intelligent Decision Technol.* (2024) 18:1–27. doi: 10.3233/IDT-230532
- Chakraborty D, Zhuang Z, Xue H, Fiecas MB, Shen X, Pan W. Deep learning-based feature extraction with MRI data in neuroimaging genetics for alzheimer's disease. *Genes.* (2023) 14:626. doi: 10.3390/genes14030626
- Asaduzzaman M, Alom MK, Karim ME. ALZENET: deep learning-based early prediction of Alzheimer's disease through magnetic resonance imaging analysis. *Telematics Inf Rep.* (2025) 17:100189. doi: 10.1016/j.teler.2025.100189
- Mahjoubi MA, Lamrani D, Saleh S, Moutaouakil W, Ouhmida A, Hamida S, et al. Optimizing ResNet50 performance using stochastic gradient descent on MRI images for Alzheimer's disease classification. *Intelligence-Based Med.* (2025) 11:100219. doi: 10.1016/j.ibmed.2025.100219
- Waldo-Benítez G, Padierna LC, Ceron P, Sosa MA. Dementia classification from magnetic resonance images by machine learning. *Neural Computing Appl.* (2024) 36:2653–64. doi: 10.1007/s00521-023-09163-y
- Awang MK, Rashid J, Ali G, Hamid M, Mahmoud SF, Saleh DI, et al. Classification of Alzheimer disease using DenseNet-201 based on deep transfer learning technique. *PloS One.* (2024) 19:e0304995. doi: 10.1371/journal.pone.0304995
- Shaffi N, Subramanian K, Vimbi V, Hajamohideen F, Abdesselam A, Mahmud M. Performance evaluation of deep, shallow and ensemble machine learning methods for the automated classification of alzheimer's disease. *Int J Neural Syst.* (2024) 34:2450029. doi: 10.1142/S0129065724500291
- de Mori A, Tauber C, A. S. D. N. Initiative. Longitudinal dementia trajectories for Alzheimer's Disease characterization and prediction. *Comput Biol Med.* (2025) 192:110241. doi: 10.1016/j.combiomed.2025.110241
- Singh PK, Upadhyay PK. An intuitive distributional random forest technique for dementia severity class detection. *Iran J Comput Sci.* (2025), 1–17. doi: 10.1007/s42044-025-00268-2
- Islam M, Hasan MJ, Mahdy M. CQ-CNN: A lightweight hybrid classical-quantum convolutional neural network for Alzheimer's disease detection using 3D structural brain MRI. *PloS One.* (2025) 20:e0331870. doi: 10.1371/journal.pone.0331870